A Novel Modal Decomposition Control and Its Application to PSS Design for Damping Interarea Oscillations in Power Systems

Junbo Zhang, *Student Member, IEEE*, C. Y. Chung, *Senior Member, IEEE*, and Yingduo Han, *Senior Member, IEEE*

***Abstract*—The residue method has been widely used for tuning power system stabilizers (PSSs) in large power systems to improve the damping of interarea oscillations. However, an additional PSS installation may affect the performance of existing PSSs due to interactions among different modes. When contending with several interarea oscillations, compromise among different modes becomes necessary. In this paper, a novel method based on modal decomposition is proposed for tuning PSSs for damping of the concerned interarea mode, while minimizing its effect on other modes by weakening the interactions among different modes. Design considerations, PSS structure and tuning procedure are formulated. The performance of the proposed method has been validated based on a two-area four-machine system and an actual large power system, China Southern Grid.**

***Index Terms*—Interarea low frequency oscillation, modal decomposition, power system stabilizer (PSS), residue methods, small signal stability.**

I. Introduction

POWER systems' low frequency oscillation is one of the most frequently encountered problems in small signal stability [1]. Typically, low frequency oscillations are classified as local mode oscillations and interarea mode oscillations. The former is caused by interactions among a few generators close to each other with frequencies in the range of 0.7–2.0 Hz. The latter is caused by interactions among large groups of generators with frequencies in the range of 0.1–0.7 Hz. With the growth of power systems interconnections, interarea mode oscillation has become a serious limiting factor affecting transfer of power in large quantities among different areas.

Manuscript received July 28, 2011; revised November 29, 2011 and January 19, 2012; accepted February 16, 2012. Date of publication April 03, 2012; date of current version October 17, 2012. This work was supported in part by the Major Program of National Natural Science Foundation of China (51037002), the Major State Basic Research Development Program of China (2011CB302805), and the Department of Electrical Engineering of The Hong Kong Polytechnic University. Paper no. TPWRS-00702-2011.

J. Zhang is with the Department of Electrical Engineering, Tsinghua University, Beijing, China, and also with the Department of Electrical Engineering, The Hong Kong Polytechnic University, Hong Kong, China (e-mail: zhangjb04@mails.tsinghua.edu.cn).

C. Y. Chung is with the Department of Electrical Engineering, The Hong Kong Polytechnic University, Hong Kong , China (e-mail: eecychun@polyu.edu.hk).

Y. Han is with the Department of Electrical Engineering, Tsinghua University, Beijing, China (e-mail: hanyd@mail.tsinghua.edu.cn).

Color versions of one or more of the figures in this paper are available online at http://ieeexplore.ieee.org.

Digital Object Identifier 10.1109/TPWRS.2012.2188820

The most popular analysis methods in this field are the complex torque coefficients (CTC) method and the eigenvalue analysis method [2]–[7]. CTC method is mainly used to study local mode oscillation based on frequency response analysis. Interarea mode oscillation is studied by eigenvalue analysis method through linearizing the power system. Since it is difficult to formulate the full-order or detailed linear models of very large power systems, reduced order models obtained by the identification method [8]–[10] are commonly employed in control design. However, such reduced systems simplify the interactions among different modes and cause the damping control (for interarea oscillations) to perform in an unpredictable manner.

Power system stabilizer (PSS) is a classical device effective for damping low frequency oscillations [11]. The main methods for PSS tuning and application are CTC and eigenvalue methods [12]–[16]. However, the generators may have low participation in the interarea mode and, therefore, their PSSs are required to have high gain for providing sufficient damping to the interarea mode [12]. In CTC, PSSs are tuned without coordination and this may lead to strong interactions among different modes. With the proposed PSS4B [17], use of different gains and phase compensations for a wide range of frequencies is possible and that makes it possible to overcome limitations of the CTC method. However, tuning the gains and phase compensations of PSS4B involves compromises between different modes, which makes sequential tuning in large interconnected systems difficult. With development of the wide-area measurement system (WAMS), use of global signals for damping interarea oscillation enhances observability of the generator to the concerned interarea mode and thus amplifies advantages of the eigenvalue analysis method [18], [19]. However, when using the eigenvalue method, it is also quite difficult to coordinate PSSs by using the conventional phase compensation method.

This paper, therefore, proposes a modal decomposition method for PSS tuning to provide sufficient damping to the concerned interarea mode by eliminating the interactions among different modes. Since a PSS affects the concerned mode only, PSSs can be tuned sequentially and good coordination can be achieved. The proposed method is a modification of the eigenvalue analysis method and the proposed PSS can serve as a complement to the conventional PSSs.

The rest of the paper is organized as follows. Section II reviews the eigenvalue analysis method and PSS tuning based on residues, and then discusses its limitations. Section III proposes a novel modal decomposition method and applies it to PSS tuning. The PSS structure and tuning procedures are

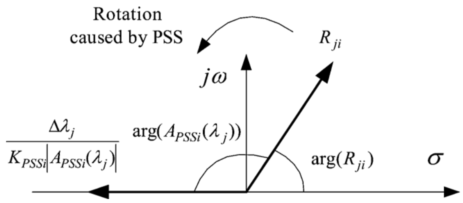

Fig. 1. Effect of residue compensation at mode j.

also described. Results of simulation of a two-area four-machine system and China Southern Grid (GSG) are reported in Sections IV and V, respectively. Section VI discusses merits and shortcomings of the proposed method, as well as future work. Section VII concludes the paper.

II. Review of Eigenvalue Analysis Method and its Application to PSS Tuning

A. Review of Eigenvalue Analysis Method

The linearized state-space model of an n-order single-input-single-output (SISO) power system is given as follows:

$$\dot{\boldsymbol{x}} = \boldsymbol{A}\boldsymbol{x} + \boldsymbol{B}_i u_i \quad (1)$$
$$y_i = \boldsymbol{C}_i \boldsymbol{x} \quad (2)$$

where $\boldsymbol{x} \in \Re^n$ is the state vector; $\boldsymbol{A}$ is the state matrix; u_i and y_i are input and output, respectively, of the ith generator; and correspondingly, $\boldsymbol{B}_i$ and $\boldsymbol{C}_i$ are input and output vectors, respectively. Thus, the following equations can hold for $\boldsymbol{A}$:

$$\boldsymbol{A}\boldsymbol{M} = \boldsymbol{M}\boldsymbol{\Lambda} \quad (3)$$
$$\boldsymbol{M}\boldsymbol{N}^T = \boldsymbol{I} \quad (4)$$

where $\boldsymbol{M}$ and $\boldsymbol{N}$ are right and left modal matrices, respectively, defined as follows:

$$\boldsymbol{M} = [\boldsymbol{m}_1, \boldsymbol{m}_2, \ldots, \boldsymbol{m}_n] \quad (5)$$
$$\boldsymbol{N} = [\boldsymbol{n}_1, \boldsymbol{n}_2, \ldots, \boldsymbol{n}_n]. \quad (6)$$

$\boldsymbol{\Lambda}$ is a diagonal matrix with the following definition:

$$\boldsymbol{\Lambda} = \mathrm{diag}(\lambda_1, \lambda_2, \ldots, \lambda_n). \quad (7)$$

Here $\lambda_1, \lambda_2, \ldots, \lambda_{\mathrm{n}}$ are eigenvalues of $\boldsymbol{A}$. Assuming the ith generator is on "open-loop", in order to stabilize the system, damping controllers should move all eigenvalues of the closed loop system to the left hand side of the complex plane.

B. PSS Design Based on Residues

The scalar transfer function is obtained as follows:

$$G_i(s) = \frac{y_i}{u_i} = \sum_{j=1}^{n} \frac{R_{ji}}{(s-\lambda_j)} \quad (8)$$

where R_{ji} is the residue with respect to the jth mode (λ_j) and it can be calculated from the following equation:

$$R_{ji} = \boldsymbol{C}_i \boldsymbol{m}_j \boldsymbol{n}_j^T \boldsymbol{B}_i. \quad (9)$$

When installing a PSS in the ith generator, the change of the jth eigenvalue is computed as follows:

$$\Delta\lambda_j = R_{ji} K_{\mathrm{PSS}i} A_{\mathrm{PSS}i}(\lambda_j) \quad (10)$$

where $K_{\mathrm{PSS}i}$ and $A_{\mathrm{PSS}i}(\lambda_j)$ are the gain and phase lead-lag compensators, respectively, of the PSS. To shift the jth mode to the left, horizontally, without changing its frequency, as shown in Fig. 1 [where $\Delta\lambda_j/(K_{PSSi}|A_{PSSi}(\Delta\lambda_j)|)$ stands for the change of the jth eigenvalue, which is proportional to gain of PSS], phase compensation of the PSS should be

$$\arg[A_{\mathrm{PSS}i}(\lambda_j)] = 180^\circ - \arg[R_{ji}]. \quad (11)$$

Therefore, the change in the real part (σ_j) of the jth mode can be calculated as

$$\Delta\sigma_j = K_{\mathrm{PSS}i}|R_{ji} A_{\mathrm{PSS}i}(\lambda_j)|. \quad (12)$$

C. Discussion

For a SISO controller, the desired phase compensation for a local or interarea mode can be accurately obtained based on the residue analysis. Thus, it may be quite effective to design a SISO damping controller by using this method [12], [17]. However, this kind of PSS affects all observable and controllable modes in the control loop even after careful tuning. For multi-input-multi-output (MIMO) controllers, phase compensation of each individual controller cannot be determined simply by the residue analysis on the scalar open loop transfer function because these controllers may strongly affect each other, especially when they work in a coordinated manner to damp interarea oscillations.

III. Proposed Modal Decomposition Control and its Application to PSS Design

As mentioned in Section II-C, although it is quite easy to apply residue information in control design, a damping controller tuned for one mode by using the conventional residue method may have negative effect on other modes. Moreover, it is rather desirable that interactions between damping controllers will be weakened when designing them for improving their respective modes. Therefore, if this is true, these damping controllers can be sequentially configured in practice, which may significantly relieve the engineers from the pressure of considering coordination between them. Based upon these considerations, a new control design method is proposed in this paper, which uses modal decomposition, introduced in detail in the following.

A. Modal Decomposition and Control Method

Define the similarity transformation as follows:

$$\boldsymbol{x} = \boldsymbol{M}\boldsymbol{z} \quad (13)$$

where $\boldsymbol{z}$ is the state vector in the new coordinate. Then, the following equation can be derived from (1):

$$\dot{\boldsymbol{z}} = \boldsymbol{M}^{-1}\boldsymbol{A}\boldsymbol{M}\boldsymbol{z} + \boldsymbol{M}^{-1}\boldsymbol{B}_i u_i = \boldsymbol{\Lambda}\boldsymbol{z} + \boldsymbol{N}^T\boldsymbol{B}_i u_i. \quad (14)$$

Moreover, based on (2), (4), and (13), it is inferred that the feedback signal is

$$y_i = \boldsymbol{C}_i \boldsymbol{M} z = \sum_{j=1}^{n} \boldsymbol{C}_i \boldsymbol{m}_j z_j. \tag{15}$$

If y_i is a sole modal signal (i.e., it consists of information of the corresponding mode only), then $y_i = \boldsymbol{C}_i \boldsymbol{m}_j z_j$, where z_j is the jth component of $\boldsymbol{z}$. Therefore, a feedback control law is formulated as

$$u_i = K_{\mathrm{PSS}i} A_{\mathrm{PSS}i}(s) y_i = K_{\mathrm{PSS}i} A_{\mathrm{PSS}i}(s) \boldsymbol{C}_i \boldsymbol{m}_j z_j \tag{16}$$

where $K_{\mathrm{PSS}i}$ and $A_{\mathrm{PSS}i}(s)$ are gain and phase lead-lag compensators, respectively, of the PSS for the ith generator. Consequently, based on (16), the state space (14) can be further formulated as

$$\begin{aligned} \dot{\boldsymbol{z}} &= \boldsymbol{\Lambda z} + \boldsymbol{N}^T \boldsymbol{B}_i K_{\mathrm{PSS}i} A_{\mathrm{PSS}i}(s) \boldsymbol{C}_i \boldsymbol{m}_j z_j \\ &= \boldsymbol{\Lambda z} + \boldsymbol{N}^T \boldsymbol{B}_i [0\ 0 \ldots K_{\mathrm{PSS}i} A_{\mathrm{PSS}i}(s) \boldsymbol{C}_i \boldsymbol{m}_j \ldots 0] \boldsymbol{z} \\ &= \boldsymbol{\Lambda} z + [\boldsymbol{0}\ \boldsymbol{0} \ldots \boldsymbol{N}^T \boldsymbol{B}_i K_{\mathrm{PSS}i} A_{\mathrm{PSS}i}(s) \boldsymbol{C}_i \boldsymbol{m}_j \ldots \boldsymbol{0}] \boldsymbol{z} \\ &= \boldsymbol{A}^* \boldsymbol{z} \end{aligned} \tag{17}$$

where $\boldsymbol{A}^*$ is the transformed system matrix (in the same dimension as that of the open loop system) with the following definition:

$$\boldsymbol{A}^* = \begin{bmatrix} \lambda_1 & 0 & \cdots & \boldsymbol{n}_1^T \boldsymbol{B}_i K_{\mathrm{PSS}i} A_{\mathrm{PSS}i}(s) \boldsymbol{C}_i \boldsymbol{m}_j & \cdots & 0 \\ 0 & \lambda_2 & \cdots & \boldsymbol{n}_2^T \boldsymbol{B}_i K_{\mathrm{PSS}i} A_{\mathrm{PSS}i}(s) \boldsymbol{C}_i \boldsymbol{m}_j & \cdots & 0 \\ \vdots & \vdots & \ddots & \vdots & \ddots & \vdots \\ 0 & 0 & \cdots & \lambda_j + \boldsymbol{n}_j^T \boldsymbol{B}_i K_{\mathrm{PSS}i} A_{\mathrm{PSS}i}(s) \boldsymbol{C}_i \boldsymbol{m}_j & \cdots & 0 \\ \vdots & \vdots & \ddots & \vdots & \ddots & \vdots \\ 0 & 0 & \cdots & \boldsymbol{n}_n^T \boldsymbol{B}_i K_{\mathrm{PSS}i} A_{\mathrm{PSS}i}(s) \boldsymbol{C}_i \boldsymbol{m}_j & \cdots & \lambda_n \end{bmatrix}. \tag{18}$$

Besides, eigenvalues of the closed loop system can also be obtained by solving the following equation:

$$\det(s\boldsymbol{I} - \boldsymbol{A}^*) = 0. \tag{19}$$

It can be observed that eigenvalues of the open loop system $(\lambda_1, \lambda_2, \ldots, \lambda_{\mathrm{n}})$, except the jth one, are the same as those of the closed loop system, and eigenvalues of the rest of the closed loop system can be derived by solving the following equation:

$$s - \lambda_j - \boldsymbol{n}_j^T \boldsymbol{B}_i K_{\mathrm{PSS}i} A_{\mathrm{PSS}i}(s) \boldsymbol{C}_i \boldsymbol{m}_j = 0. \tag{20}$$

From inferences shown above, it is known that if the control signal contains only the jth mode, the feedback control law (16) will alter only this mode and have no effect on other modes of the open loop system. If the control input is the sole modal signal, gain and phase compensation of the controller can be determined by using the eigenvalue sensitivity technique, shown in the following.

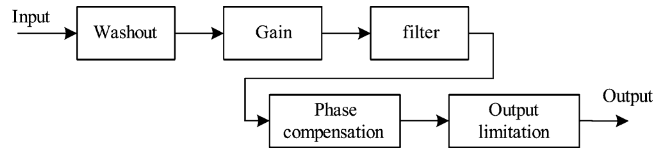

Fig. 2. Structure of the proposed PSS.

By differentiating both sides of (20) with respect to $K_{\mathrm{PSS}i}$, the following equation can be obtained:

$$\begin{aligned} \frac{\partial s}{\partial K_{\mathrm{PSS}i}} &= \boldsymbol{n}_j^T \boldsymbol{B}_i A_{\mathrm{PSS}i}(s) \boldsymbol{C}_i \boldsymbol{m}_j \\ &\quad + \boldsymbol{n}_j^T \boldsymbol{B}_i K_{\mathrm{PSS}i} \boldsymbol{C}_i \boldsymbol{m}_j \frac{\partial A_{\mathrm{PSS}i}(s)}{\partial s} \frac{\partial s}{\partial K_{\mathrm{PSS}i}}. \end{aligned} \tag{21}$$

Furthermore, it can be observed from (20) and (21) that when $K_{\mathrm{PSS}i} = 0$ (the system is open loop) and $s = \lambda_j$ (i.e., an eigenvalue of the system), the eigenvalue sensitivity with respect to $K_{\mathrm{PSS}i}$ can be obtained as follows:

$$\frac{\partial s}{\partial K_{\mathrm{PSS}i}} = \boldsymbol{n}_j^T \boldsymbol{B}_i A_{\mathrm{PSS}i}(\lambda_j) \boldsymbol{C}_i \boldsymbol{m}_j. \tag{22}$$

Therefore, phase compensation of the PSS can be calculated by using (22). Furthermore, based on (9), it is noted that the compensation phase is exactly the same as (11). Finally, the PSS gain can be increased gradually to enhance damping of the mode.

B. PSS Design Based on the Proposed Method to Damp Interarea Oscillation

The key to applying the proposed method is obtaining a pure sole modal signal. In our view, a fine tuned filter can preserve the concerned mode while annihilating other modes in the refined signal, which can approximate a sole modal signal in practical applications. Theoretically, with an ideal filter, any signal which is able to sufficiently observe the concerned mode can be chosen as the feedback control signal, such as rotor speed, bus frequency, transmission line power and/or their combinations. However, an actual filter always has spectral leakage, so it is necessary to prepare a suitable signal to help enhance the performance of the filter.

A basic requirement for the filtered signal is that it should have relatively large energy of the concerned mode. For large system with many PMUs, it is ideal to combine several signals, with the help of mode shape analysis, and average them to reduce energy of other modes.

Thus, by filtering and careful selection, the PSS, using a mostly pure modal signal as input, will have very little effect on other modes. The structure of the proposed PSS for damping interarea oscillation has the conventional structure, with an additional filter (Fig. 2).

To optimize the control results, location of PSS, i.e., the generator to be equipped, should have high controllability to the concerned mode. Several ways of choosing the feedback control loop have been suggested in extant literature [20], [21] and, therefore, we skip this part.

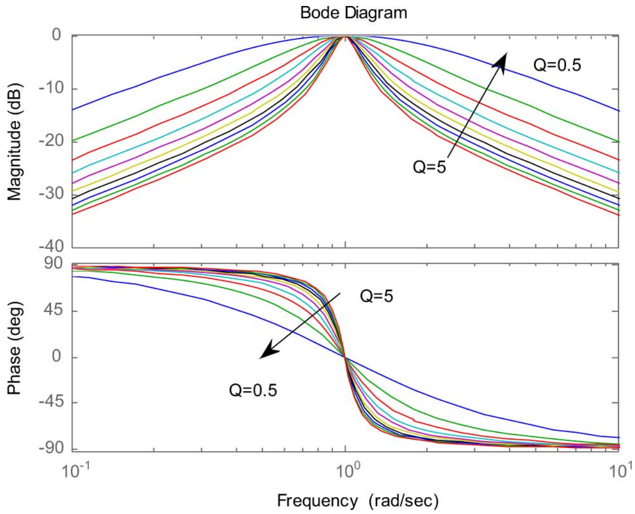

Fig. 3. Typical frequency characteristic with fixed $\omega_0 = 1$ and various values of Q, from 0.5 to 5.

C. Filter Design for Single Mode

Many researchers have proposed different designs of digital and analog filters [22]. We find that a simple second order band pass filter satisfies the demand, with transfer function

$$F(s) = \frac{\left(\frac{\omega_0}{Q}\right) s}{s^2 + \left(\frac{\omega_0}{Q}\right) s + \omega_0^2} \tag{23}$$

where ω_0 is the center frequency of the filter and Q is its quality factor.

When the center frequency is fixed, the quality factor determines the pass band. A higher Q leads to a narrow pass band and a steeper slope of the frequency, and vice versa. So when choosing Q for the PSS, there will be a compromise between pass band and the filtering effect. Fig. 3 shows a typical frequency characteristic with fixed $\omega_0 = 1$ and various values of Q.

Note that the center frequency of the filter should follow the frequency of the concerned mode. In large systems, frequency of the mode may be obtained by identification. So Q should not be so large as to endure the deviation from identification. Another notation for Q selection is that the phase at other frequencies is different from the desired phase. This may cause an unexpected change in other modes when both high Q and high gain are employed. So Q should be compromised, in order to maintain robustness. When a satisfactory damping of the concerned mode is obtained, the gain should be as small as possible.

D. PSS Tuning Procedure

The procedure of PSS tuning can be summarized in the following steps:

S.1) Determine the concerned mode and obtain its frequency and damping ratio. This is usually accomplished by small signal stability analysis or system identification, in large power systems.

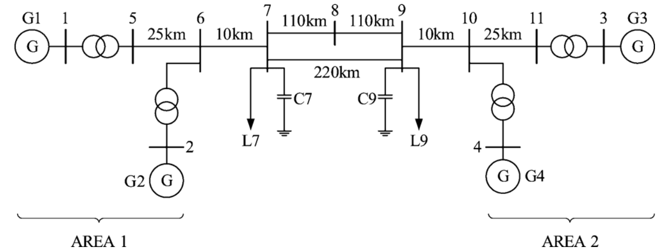

Fig. 4. Two-area four-machine system.

S.2) Select suitable location and input signal for the PSS in accordance with Section III-B.

S.3) Design the filter, with specified satisfactory quality and pass band, in accordance with Section III-C.

S.4) Calculate the suitable phase compensation for the PSS from (11). Note that as the filter is not ideal, a fine adjustment may be needed to maintain the mode's frequency without large variations. If the mode's frequency drops, the compensation phase should be smaller than (11), and vice versa.

S.5) Determine the gain of the PSS. Note that for higher gains the mode shift is no longer proportional to the gain. To guarantee the mode is shifted horizontally to the left, without change of frequency, the gain should be maintained in the linear area proportional to the modal shifting; lower gain is preferable if satisfactory damping is already obtained. In an actual system, the gain will be compromised because of limitations of PSS output, sensitivity of other modes, time delays in global signals and other practical considerations.

As the PSS changes only the concerned mode, the same procedure can be sequentially applied to tune other PSSs.

E. Discussion

Obviously the proposed modal decomposition control will perform better than the conventional residue method, though it requires a well-designed mode filter and proper signal selection. PSS designed based on this method for damping interarea oscillation has little effect on other modes. More significantly, it allows engineers to sequentially tune the PSSs to suppress multi-mode interarea oscillations without the need to consider coordination.

IV. Simulation on Two-Area Four-Machine System

A. System Introduction

A two-area four-machine system (Fig. 4) is used to validate the proposed method [1]. The system is also employed in the Simulink/Matlab for PSS performance demonstration, and all parameters are the same as in [23].

By linearizing the system around the equilibrium point, three electromechanical modes are obtained (Table I). The first is the interarea mode, poorly damped, with Generators 1 and 2 of Area 1 swinging against Generators 3 and 4 of Area 2. The other two are local modes with satisfactory damping ratios. Local mode 1

TABLE I
INTERAREA AND LOCAL MODES WITHOUT PSS

Mode name	Eigenvalue	Frequency (Hz)	Damping ratio (%)
Interarea mode	-0.0108±j4.0022	0.6370	0.2710
Local mode 1	-0.6808±j7.0481	1.1217	9.6146
Local mode 2	-1.4984±j7.4785	1.1902	19.6461

is the oscillation between Generators 1 and 2 in Area 1 and local mode 2 is the oscillation between Generators 3 and 4 in Area 2.

B. PSS Design

The aim of this study is to enhance the damping ratio of the interarea mode. For simplicity and symmetry of this system, without losing generality, the PSS is selected to be installed at Generator 1; the feedback control signal is its rotor speed, which has large energy of the interarea mode. Two PSS tuning methods are studied:

1) PSS tuning using the conventional residue method (RPSS); and
2) PSS tuning based on the proposed modal decomposition control method (FPSS, F stands for the filter).

A residue analysis shows that the phase compensation for interarea mode is about 21 degrees, and for local mode 1, it is about 43 degrees. A compensator is then designed, based on the two modes. For filter design, ω_0 is 4.187 rad/s, and Q is set as 2. In order to enable comparison, the two PSSs are assumed to have same gain at the frequency of the interarea mode (here the gain is calculated from the complex value of the PSS transfer function at $s = \mathrm{j}\omega$; and as the mode is poorly damped, it is approximately equal to the complex value at the complex modal frequency, $\lambda = \sigma + \mathrm{j}\omega$). Moreover, output limits are set to be ± 0.05 p.u. Transfer functions of RPSS and FPSS with gain 10 are

$$H_R(s) = 10\frac{10s}{1+10s}\left(\frac{1+0.0824s}{1+0.0303s}\right)^2 \tag{24}$$

$$H_F(s) = \frac{2.0935s}{s^2+2.0935s+17.5310}H_R(s). \tag{25}$$

The modes after control are shown in Table II. Because Generator 1 does not participate in local mode 2, its modal information is not provided. It can be observed that when PSS gain gradually increases from 5 to 20, FPSS always performs better than the RPSS in damping of interarea mode. As Generator 1 greatly participates in local mode 1, the RPSS enhances this mode significantly since its phase compensation covers a wide range of frequencies while FPSS leaves this mode almost unchanged. However, when the local mode is satisfied with no PSS, further increase in damping ratio has little influence on the system's stability.

A three-phase to ground fault occurs at Bus 8 at 1 s and then is cleared 120 ms later. Oscillations of the power transmitted between the two areas are shown in Fig. 5, which shows that the FPSS has better performance.

The PSS outputs are shown in Fig. 6. It is clear that the FPSS has smaller output than RPSS, with the same gain. This is because besides controlling the interarea mode, the RPSS has control effort at higher frequencies. When PSS gain is 10, the RPSS has already hit the limit, while FPSS hits the limit only when the

TABLE II
DAMPING ENHANCEMENT COMPARISON WITH DIFFERENT PSS GAIN

PSS Type	Gain	Inter–area mode		Local mode 1	
		Frequency (Hz)	Damping ratio (%)	Frequency (Hz)	Damping ratio (%)
No PSS	0	0.6370	0.2710	1.1217	9.6146
RPSS	5	0.6376	1.9906	1.1283	16.3052
	7.5	0.6384	2.7758	1.1266	19.6834
	10	0.6395	3.5110	1.1223	23.0480
	12.5	0.6408	4.1958	1.1154	26.4693
	15	0.6424	4.8295	1.1053	29.9334
	20	0.6463	5.9417	1.0763	36.8823
FPSS	5	0.6354	2.1264	1.1552	9.5386
	7.5	0.6352	3.1276	1.1715	9.4801
	10	0.6356	4.1896	1.1874	9.4111
	12.5	0.6370	5.3104	1.2031	9.3337
	15	0.6400	6.4402	1.2185	9.2496
	20	0.6515	7.9916	1.2486	9.0681

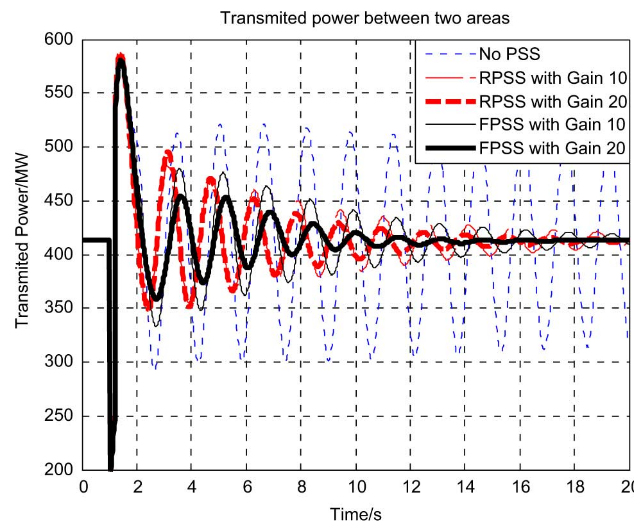

Fig. 5. Transmitted power between the two areas.

gain is 20. Therefore, FPSS is more suitable for damping the interarea mode when the control output is limited, which implies its suitability for very large systems with less PSS output.

C. Robustness Test

The robustness of the PSS to a concerned mode implies that the compensation phase of the PSS can maintain satisfaction over a range, generally ± 30 degrees, when the system operates over a wide range of normal and outage conditions. Without the filter, the proposed PSS is the same as the conventional RPSS, and has robustness over a wide range of frequency. With the filter, if Q is properly chosen, the additional phase of the filter varies within 30 degrees even when the center frequency varies $\pm 10\%$. For a system that operates over a wide range of normal conditions, there is rarely a situation where a mode frequency varies beyond $\pm 10\%$, especially for interarea modes in large power systems [24]. Therefore, the FPSS can provide robust damping to the mode. Moreover, with development of online mode estimation [25]–[28], the center frequency of the filter can be tuned adaptively according to the result of mode estimation. Then the phase compensation at the concerned mode is exactly the same as the RPSS, and provides satisfactory damping even

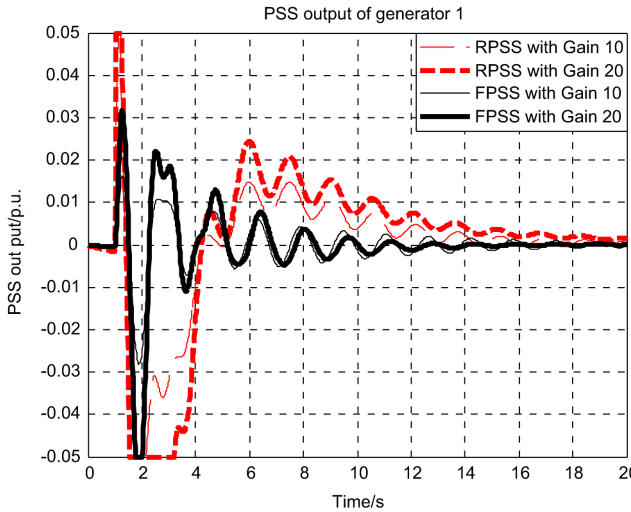

Fig. 6. Outputs of PSSs during the oscillations.

TABLE III
INTERAREA MODE IN THE ROBUSTNESS TEST RESULTS

PSS Type	Case	Frequency (Hz)	Damping ratio (%)
No PSS	Case 1	0.6294	-0.8750
	Case 2	0.6370	0.2710
	Case 3	0.6509	1.5246
RPSS	Case 1	0.6414	6.5534
	Case 2	0.6463	5.9417
	Case 3	0.6573	5.8709
FPSS	Case 1	0.6588	9.4236
	Case 2	0.6515	7.9916
	Case 3	0.6607	6.9543

with large frequency changes (under serious system outages or huge structural changes).

To validate the robustness of the FPSS, simulation is carried out. For symmetry of this system, the power transmitted between the two areas is changed for the following three cases:

Case 1: 213 MW transmitted from Area 1 to Area 2.

Case 2: 413 MW transmitted from Area 1 to Area 2, which is the original case (Section IV-B).

Case 3: 613 MW transmitted from Area 1 to Area 2.

In all the cases, RPSS and FPSS on Generator 1 are the same as in Section IV-B, with gain 20.

Table III shows results of small signal stability analysis of the interarea mode. Because of space constraints, time domain curves, which are the same as the small signal analysis results, are not provided here, and in the following sections. It can be observed that in all cases, FPSS performs better than the RPSS and its robustness is satisfactory.

D. Discussion About the Input Signals

Careful selection and combination of global signals can help enhance performance of PSSs (Section III-B). This is discussed in the following.

For symmetry of the system, we investigate rotor speed $\Delta\omega_1$ of Generator 1 and rotor speed $\Delta\omega_3$ of Generator 3. By mode shape analysis (Fig. 7), it is clear that Generators 1 and 2 are swinging against Generators 3 and 4. The input signal is set as $(\Delta\omega_1 - \Delta\omega_3)$. For comparison with $\Delta\omega_1$, the averaged signal,

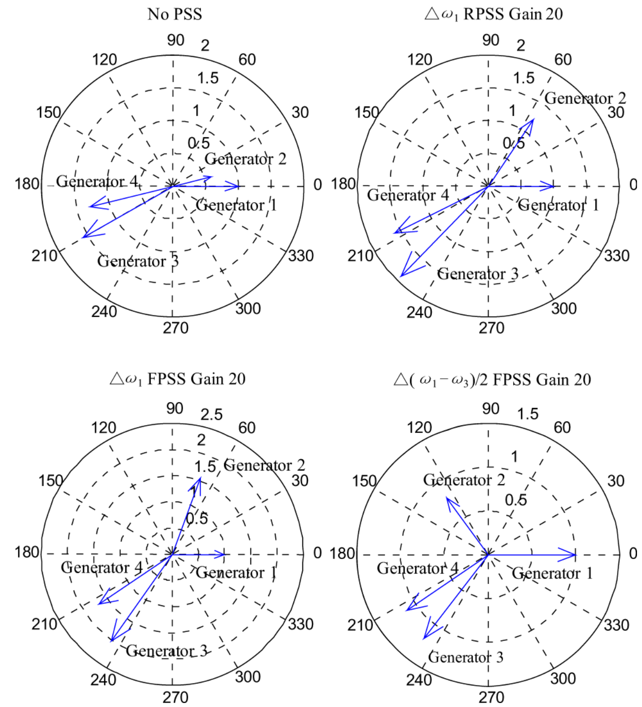

Fig. 7. Mode shape characteristics of rotor speeds of the interarea mode.

TABLE IV
COMPARISON OF DAMPING ENHANCEMENT WITH DIFFERENT PSS SIGNALS

PSS Type	Gain	Inter–area mode		Local mode 1	
		Frequency (Hz)	Damping ratio (%)	Frequency (Hz)	Damping ratio (%)
No PSS	0	0.6370	0.2710	1.1217	9.6146
$\Delta\omega_1$ FPSS	10	0.6356	4.1896	1.1874	9.4111
	20	0.6515	7.9916	1.2486	9.0681
$(\Delta\omega_1$-$\Delta\omega_3)/2$ RPSS	10	0.6296	4.4498	1.1268	15.4469
	20	0.6262	8.4325	1.1978	20.4716
$(\Delta\omega_1$-$\Delta\omega_3)/2$ FPSS	10	0.6257	5.5196	1.1502	9.4141
	20	0.5773	11.9510	1.1791	9.2191

$(\Delta\omega_1 - \Delta\omega_3)/2$, is used as the final input signal for PSS, which preserves the energy of the interarea mode and reduces the energy of the local modes.

For the new feedback control loop, the residue phase of the interarea mode is 2 degrees and the local mode is 46 degrees. Because compensation phase for either of the modes is not changed much, transfer function of RPSS is the same as in (24), while filter of FPSS is redesigned, as in (26), with the central frequency slightly changed to 4 rad/s:

$$F(s) = \frac{2s}{s^2 + 2s + 16}. \tag{26}$$

Results of eigenvalue analysis in Table IV show that with the global pure modal signal, RPSS can do better in damping interarea oscillations. However, with a well-designed filter, FPSS can do even better with the pure modal signal.

The mode shape analysis is employed again to investigate the influence of the PSSs. Fig. 7 shows that with local signal, the FPSS and RPSS have similar influences on the modal shape, which demonstrates that the filter does not have any extra effect. As the damping provided by FPSS is larger, the angle between

TABLE V
COMPARISON BETWEEN DAMPING INTERAREA MODE BY DIFFERENT PSSS

PSS Type	Gain	Inter–area mode		Local mode 1	
		Frequency (Hz)	Damping ratio (%)	Frequency (Hz)	Damping ratio (%)
No PSS	0	0.6370	0.2710	1.1217	9.6146
$\Delta\omega_1$ PSS4B	10	0.6362	3.2697	1.1750	23.6278
	20	0.6400	5.9733	1.3189	35.8332
$\Delta\omega_1$ CPSS	10	0.6409	1.9041	1.1664	14.4443
	20	0.6453	3.2318	1.2159	19.1696
$\Delta\omega_1$ RPSS	10	0.6395	3.5110	1.1223	23.0480
	20	0.6463	5.9417	1.0763	36.8823
$\Delta\omega_1$ FPSS	10	0.6356	4.1896	1.1874	9.4111
	20	0.6515	7.9916	1.2486	9.0681
$(\Delta\omega_1$-$\Delta\omega_3)/2$ FPSS	10	0.6257	5.5196	1.1502	9.4141
	20	0.5773	11.9510	1.1791	9.2191

Generators 1 and 2 is larger. With global signal, FPSS provides the largest damping, and leads to the largest angle between Generators 1 and 2. An interesting pattern is that the higher is the damping a PSS provides, the larger is the angle between Generators 1 and 2. When the gain of a PSS increases gradually, this pattern is shown clearly. The same pattern is obvious on RPSS with global signal also. For the sake of brevity, extra plots are not shown here.

E. Further Comparisons

The last comparison is between different types of PSSs. Here we add two other kinds of PSSs:

1) PSS4B, which is the same as in [17]; and
2) conventional PSS (CPSS) tuned by GEP method from [1].

The parameters, block settings and frequency responses of the two PSSs can be directly obtained from [23]. In order to enable comparison, all PSSs are with the same gains as 10 and 20 at the interarea mode and their output limits are set to be ± 0.05 p.u. Results of the small signal stability analysis are shown in Table V.

It is clear when all PSSs are with the same gain at the interarea mode, with local signal $\Delta\omega_1$, PSS4B and RPSS have similar results in damping the interarea mode, while CPSS does not perform as well as the other PSSs; and with local signal $\Delta\omega_1$ and global signal $(\Delta\omega_1 - \Delta\omega_3)/2$, FPSS gets even better results. This is because with limited effect, FPSS can focus on the interarea mode, while the other PSSs are influenced by interactions between local and interarea modes. The best performance is by FPSS with global signal $(\Delta\omega_1 - \Delta\omega_3)/2$, which validates the notion that the proposed modal decomposition control is more suitable for damping interarea oscillations, especially when PSS is with low gain and small output limits.

V. SIMULATION ON AN ACTUAL LARGE POWER SYSTEM

A. System Introduction

China Southern Grid (CSG) is one of the two bulk AC synchronized power networks in China, comprising Guangdong (GD), Guangxi (GX), Yunnan (YN), Guizhou (GZ), and Hainan (HN) provincial networks (Fig. 8). CSG is also known as one of the largest AC/DC parallel transmission systems in the world. More than 18 GW of power is transmitted from YN and GZ to load centers in GD through an AC/DC hybrid transmission corridor. The transmission corridor, also known as the "west-to-east-corridor", consists of eight 500-kV AC links and four $\pm$500-kV DC links.

The interarea low frequency oscillation is one of the key problems that limit CSG's power transfer capacity from west to east. Oscillation events on September 1, 2005, August 29, 2006, and April 21, 2008 highlighted the need to improve damping of interarea oscillations.

The simulation environment is chosen on the basis of operating conditions prevailing in 2009. No wide-area damping controller for HVDC links is assumed. The entire network includes 570 generators, 4046 buses, 2027 AC lines, 4 HVDC lines, and numerous system devices and controllers.

B. Feedback Control Loop Selection

There are two interarea modes in this system, the YN versus GZ mode, and the (YN and GZ) versus GD mode. The YN versus GZ mode dominates oscillations of generators between Yunnan and Guizhou provinces with a typical frequency of about 0.58 Hz while the (YN and GZ) versus GD mode dominates oscillation of Yunnan and Guizhou provinces against Guangdong province, with a typical frequency of about 0.38 Hz. In this case, most generators are equipped with conventional local PSSs. Although the (YN and GZ) versus GD mode is well damped by coordinated control of HVDC and PSSs [29], [30], the YN versus GZ mode is still poorly damped. We introduce two wide-area PSSs to enhance damping ratios. This can be treated as a standard procedure for MIMO sequential PSSs tuning.

Primary signal analysis shows that wide-area signals such as bus frequencies from Anshun, Xingren in Guizhou province and Chuxiong, Qujing in Yunnan province (which can be found in Fig. 8) have high observability in the poorly damped YN versus GZ mode. They also have a component of (YN and GZ) versus GD mode and other local modes. Analyzing of the mode shape (Fig. 9) shows that Anshun and Xingren are opposite of Chuxiong and Qujing. Following Section IV-D, we combine these signals according to their modal shape directions, and then average them by 4. The final input signal for the wide-area PSS is (Anshun + Xingren-Chuxiong-Qujing)/4.

Then we select the locations for the PSSs. The Xiaowan station located in the west of Yunnan province has the highest residue with respect to the YN versus GZ mode, so it is selected as the first location for PSS installation. The Goupitan station located in the east of Guizhou province also has a high residue with respect to the YN versus GZ mode, so it is selected as the second location for PSS installation.

C. PSS Design

The objective of wide-area PSSs is to damp oscillation of the YN versus GZ mode. The center frequency is set at 0.58 Hz and the quality factor Q is set at 2. Output limits of wide-area PSSs are set to be ± 0.1 p.u.

Two kinds of PSSs have been compared, as follows:

1) Wide-area PSS tuned by the residue method (RPSS); and
2) Wide-area PSS tuned by the proposed method (FPSS).

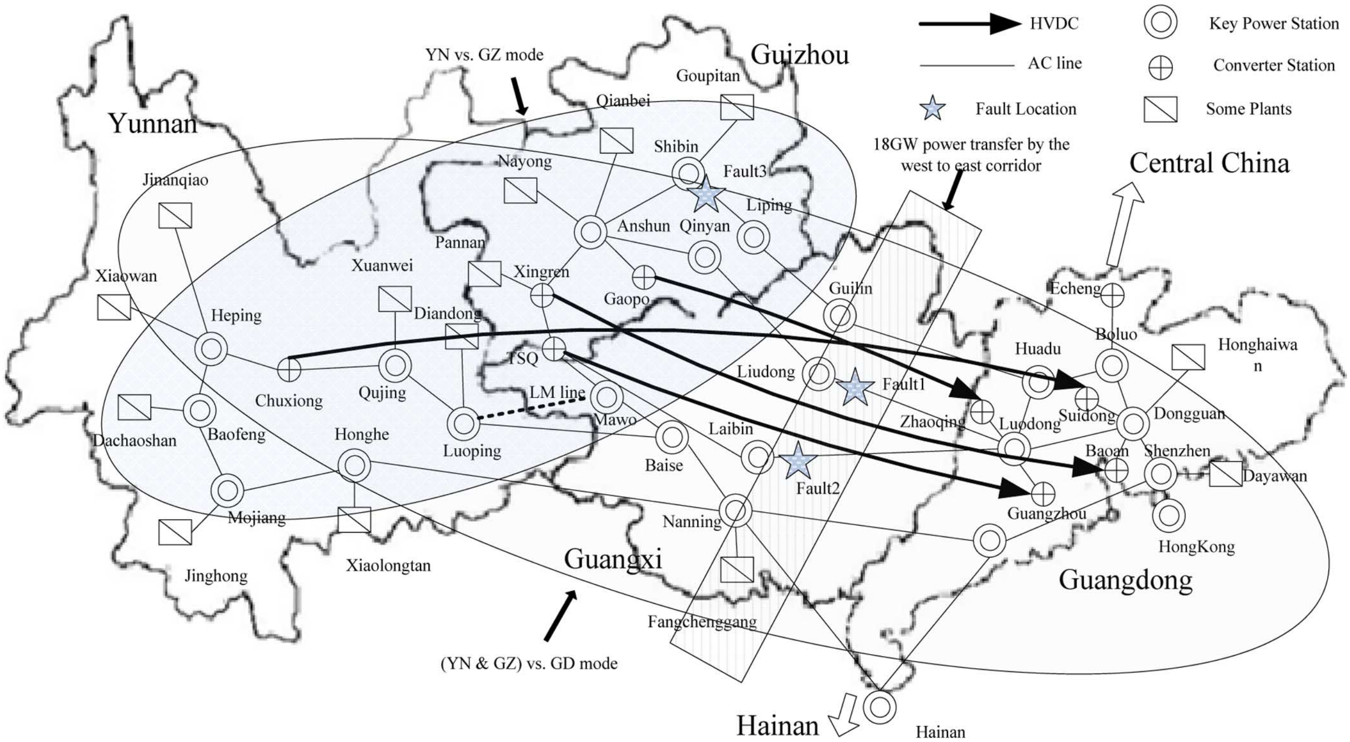

Fig. 8. China Southern Grid in 2009.

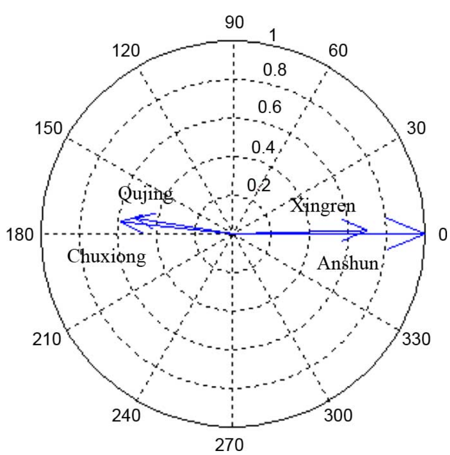

Fig. 9. Mode shape characteristics of the input signals of the YN versus GZ mode.

According to the method proposed in Section III-D, the appropriate phase compensations for wide-area PSSs are about 30 degree in Xiaowan and 45 degree in Goupitan, and the phase compensation blocks are designed accordingly. The gain is set at 6 p.u. since larger gains offer no significant improvements; output of the PSS hits the limit.

For comparison, the residue method is used to tune the PSS in Xiaowan station as well. The transfer functions of these PSSs are obtained as follows (Subscript 1 for Xiaowan and 2 for Goupitan):

$$H_{R1}(s) = 6\frac{10s}{1+10s}\left(\frac{1+0.2s}{1+0.13s}\right)^3 \tag{27}$$

$$\begin{aligned} H_{F1}(s) &= 6\frac{10s}{1+10s}\frac{1.76s}{12.2+1.76s+s^2} \\ &\quad \times \left(\frac{1+0.2s}{1+0.13s}\right)^3 \end{aligned} \tag{28}$$

$$\begin{aligned} H_{F2}(s) &= 6\frac{10s}{1+10s}\frac{1.76s}{12.2+1.76s+s^2} \\ &\quad \times \left(\frac{1+0.22s}{1+0.12s}\right)^3. \end{aligned} \tag{29}$$

D. Simulations

Three-phase short circuit faults occur at three different locations in the system:

Fault 1 occurs at Liudong side of the transmission line between Liudong and Luodong. This line is an important part of the west-to-east transmission corridor. The fault is one of the most serious faults experienced and excites both interarea modes.

Fault 2 occurs at Laibin side of the transmission line between Laibin and Luodong. The line is a part of the southern west-to-east transmission corridor, and the fault excites the (YN and GZ) versus GD mode and some local modes.

Fault 3 occurs at Shibin side of the transmission line between Shibin and Liping. This line is a part of northern west-to-east transmission corridor, and the fault excites the YN and GZ mode and some local modes.

During each fault, four simulations are carried out:

Case 1: No wide-area PSS in this system.

Case 2: PSS tuned by the residue method in Xiaowan station.

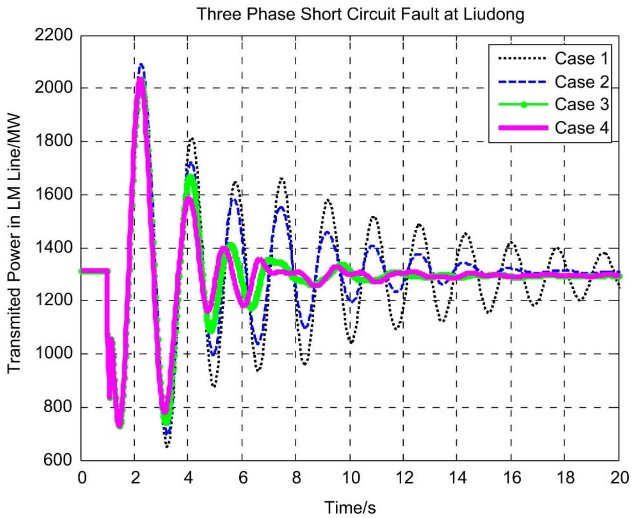

Fig. 10. Power oscillation in LM line during Fault 1.

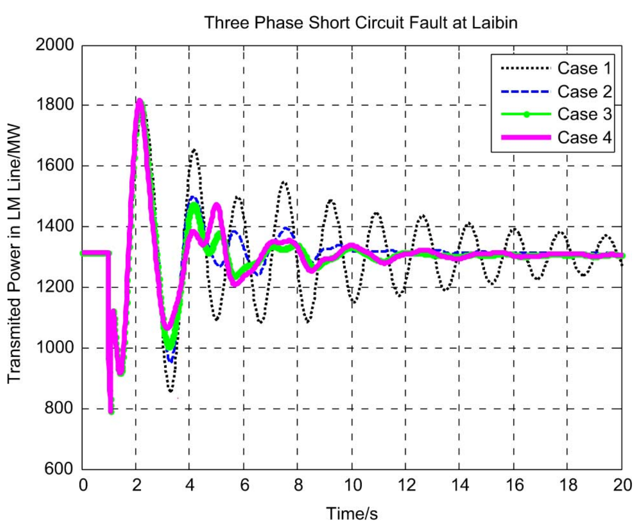

Fig. 11. Power oscillation in LM line during Fault 2.

Case 3: PSS tuned by the proposed method in Xiaowan station.

Case 4: PSSs tuned by the proposed method in Xiaowan station and Goupitan sequentially (i.e., another PSS installed in Goupitan based on Case 3 above).

Active power oscillations of LM line, which connects Luoping and Mawo stations and has high sensitivity in both modes (Fig. 8), are shown in Figs. 10–12. Moreover, the mode information (Table VI) is obtained through implementing Prony algorithm on these curves (time window between 2 to 12 s).

The simulation results show that:

1) With only conventional local PSSs, the YN versus GZ mode is poorly damped. This means conventional local PSSs are not effective in damping interarea oscillations.
2) Comparing Cases 2 and 3 of each fault, the wide-area FPSS is much more effective than wide-area RPSS for damping the concerned YN versus GZ mode.

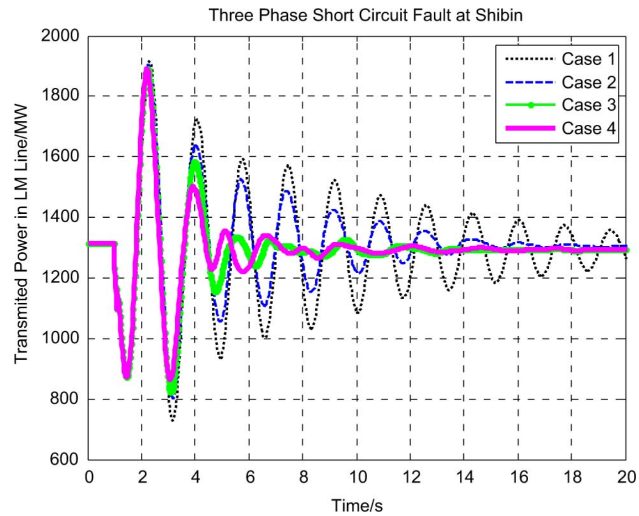

Fig. 12. Power oscillation in LM line during Fault 3.

TABLE VI
COMPARISON OF DIFFERENT PSSS IN CGS

Fault no.	Different cases	YN .vs. GZ mode		(YN & GZ) .vs. GD mode	
		Frequency (Hz)	Damping ratio (%)	Frequency (Hz)	Damping ratio (%)
1	Case 1	0.586	3.04	0.399	12.551
	Case 2	0.585	5.42	0.391	13.991
	Case 3	0.594	15.84	0.372	12.375
	Case 4	0.579	23.128	0.379	15.121
2	Case 1	0.586	2.753	0.386	13.717
	Case 2	0.586	11.05	0.362	16.186
	Case 3	0.541	34.398	0.361	13.528
	Case 4	Decays rapidly		0.374	13.905
3	Case 1	0.585	3.273	0.398	12.216
	Case 2	0.582	5.492	0.407	15.079
	Case 3	0.588	19.116	0.377	17.630
	Case 4	0.575	31.638	0.388	17.311

3) For the (YN and GZ) versus GD mode, comparing Cases 2 and 3, wide-area FPSS has effect comparable with wide-area RPSS in different faults.
4) In Case 4, each fault shows satisfactory results in both modes. This demonstrates that by sequential tuning, overall stability can be reached.
5) Note that in Case 4 of Fault 2, as the YN versus GZ mode is not highly excited, it decays rapidly in the first two seconds (after the fault) and cannot be even detected by the Prony method, using time window between 2 to 12 s. The effects of damping YN versus GZ mode are illustrated in the first swing of the oscillation (Fig. 11).

VI. FURTHER DISCUSSION

The cases in Section IV and V validate the proposed method for inhibiting a poorly damped interarea oscillation. In this section, we further discuss the merits and shortcomings of this method, and then introduce our future work, in order to establish a complete understanding.

A. Merits and Shortcomings

The proposed FPSS serves as a complement to the conventional local PSS and its application is focused on enhancing the damping to the concerned interarea mode, especially when local PSSs are unable to provide sufficient damping. However, its shortcoming is that it provides no extra damping to other modes.

Since the filter minimizes interactions among different modes, interactions among different control loops are minimized as well, which benefits the sequential tuning.

Further, by eliminating the FPSS's interactions with other modes, it is convenient to employ and can coordinately work with conventional local PSSs (employed and validated in Section V), to provide overall stability in large power systems.

B. Future Work

With development of the online mode estimation, it is possible to develop an adaptive FPSS (the center frequency of the filter can be adaptively tuned, according to the mode estimation). The next step of our research work is to find out how to connect both techniques in practice. More surveys will be conducted about time delay in transmission of wide-area signals in the future.

VII. Conclusions

In this paper, a modal decomposition control approach is proposed and applied to design PSS for interarea oscillation inhibition. The proposed method reduces limitations of the existing residue method by alleviating interactions between the concerned mode and other modes. Simulation results of the two cases validate the proposed method. The first two-area four-machine case shows the advantages of the proposed method, compared to the conventional residue method. FPSS tuning by the proposed method enhances damping ratio of the interarea mode with smaller control effect than RPSS tuning by the conventional residue method. The robustness test shows that it works well in different system conditions. The second case in CSG shows the application procedure of an actual complex system. It can be pointed out that by proper coordinated control with local PSS and wide-area FPSS, overall stability can be achieved.

Acknowledgment

The authors would like to thank Mr. D. P. Ke of The Hong Kong Polytechnic University and Dr. Chao Lu and Miss Yi Zhao from Tsinghua University for their constructive help.

References

[1] P. Kundur, *Power System Stability and Control*. New York: McGraw-Hill, 1994.

[2] F. P. Demello and C. Concordia, "Concepts of synchronous machine stability as affected by excitation control," *IEEE Trans. Power App. Syst.*, vol. PAS-88, no. 4, pp. 316–329, Apr. 1969.

[3] G. Gross, C. F. Imparato, and P. M. Look, "A tool for the comprehensive analysis of power system dynamic stability," *IEEE Trans. Power App. Syst.*, vol. PAS-101, no. 1, pp. 226–234, Jan. 1982.

[4] N. Martins, "Efficient eigenvalue and frequency response methods applied to power system small-signal stability studies," *IEEE Trans. Power Syst.*, vol. 1, no. 1, pp. 217–224, Feb. 1986.

[5] P. Kundur, M. Klein, G. J. Rogers, and M. S. Zywno, "Application of power system stabilizers for enhancement of overall system stability," *IEEE Trans. Power Syst.*, vol. 4, no. 2, pp. 614–626, May 1989.

[6] F. L. Pagola, I. J. Perez-Arriaga, and G. C. Verghese, "On sensitivities, residues and participations: Applications to oscillatory stability analysis and control," *IEEE Trans. Power Syst.*, vol. 4, no. 1, pp. 278–285, Feb. 1989.

[7] C. Y. Chung, L. Wang, F. Howell, and P. Kundur, "Generation rescheduling methods to improve power transfer capability constrained by small-signal stability," *IEEE Trans. Power Syst.*, vol. 19, no. 1, pp. 524–530, Feb. 2004.

[8] I. Kamwa and L. Gerin-Lajoie, "State-space system identification-toward MIMO models for modal analysis and optimization of bulk power systems," *IEEE Trans. Power Syst.*, vol. 15, no. 1, pp. 326–335, Feb. 2000.

[9] A. Hasanovic, A. Feliachi, N. B. Bhatt, and A. G. DeGroff, "Practical robust PSS design through identification of low-order transfer functions," *IEEE Trans. Power Syst.*, vol. 19, no. 3, pp. 1492–1500, Aug. 2004.

[10] N. Zhou, J. W. Pierre, and J. F. Hauer, "Initial results in power system identification from injected probing signals using a subspace method," *IEEE Trans. Power Syst.*, vol. 21, no. 3, pp. 1296–1302, Aug. 2006.

[11] E. V. Larsen and D. A. Swann, "Applying power system stabilizers, Part I–III," *IEEE Trans. Power App. Syst.*, vol. PAS-100, no. 6, pp. 3017–3024, Jun. 1981.

[12] M. J. Gibbard and D. J. Vowles, "Reconciliation of methods of compensation for PSSs in multimachine systems," *IEEE Trans. Power Syst.*, vol. 19, no. 1, pp. 463–472, Feb. 2004.

[13] C. Y. Chung, K. W. Wang, C. T. Tse, and R. Niu, "Power-system stabilizer (PSS) design by probabilistic sensitivity indexes (PSIs)," *IEEE Trans. Power Syst.*, vol. 17, no. 3, pp. 688–693, Aug. 2002.

[14] C. Y. Chung, K. W. Wang, C. T. Tse, X. Y. Bian, and A. K. David, "Probabilistic eigenvalue sensitivity analysis and PSS design in multimachine systems," *IEEE Trans. Power Syst.*, vol. 18, no. 4, pp. 1439–1445, Nov. 2003.

[15] R. A. Jabr, B. C. Pal, and N. Martins, "A sequential conic programming approach for the coordinated and robust design of power system stabilizers," *IEEE Trans. Power Syst.*, vol. 25, no. 3, pp. 1627–1637, Aug. 2010.

[16] D. P. Ke, C. Y. Chung, and Y. Xue, "An eigenstructure-based performance index and its application to control design for damping interarea oscillations in power systems," *IEEE Trans. Power Syst.*, vol. 26, no. 4, pp. 2371–2380, Nov. 2011.

[17] I. Kamwa, R. Grondin, and G. Trudel, "IEEE PSS2B versus PSS4B: The limits of performance of modern power system stabilizers," *IEEE Trans. Power Syst.*, vol. 20, no. 2, pp. 903–915, May 2005.

[18] M. E. Aboul-Ela, A. A. Sallam, J. D. McCalley, and A. A. Fouad, "Damping controller design for power system oscillations using global signals," *IEEE Trans. Power Syst.*, vol. 11, no. 2, pp. 767–773, May 1996.

[19] I. Kamwa, R. Grondin, and Y. Hebert, "Wide-area measurement based stabilizing control of large power systems-a decentralized/hierarchical approach," *IEEE Trans. Power Syst.*, vol. 16, no. 1, pp. 136–153, Feb. 2001.

[20] A. Heniche and I. Kamwa, "Assessment of two methods to select wide-area signals for power system damping control," *IEEE Trans. Power Syst.*, vol. 23, no. 2, pp. 572–581, May 2008.

[21] H. Jingbo, L. Licheng, C. Huixiang, W. Xiaochen, and L. Peng, "Selection of feedback signal for power system damping controller based on wide area measurements," *Automat. Elect. Power Syst.*, vol. 31, no. , 9, pp. 6–10, 2007.

[22] Thede and Les, *Practical Analog and Digital Filter Design*. Boston, MA: Artech House, 2004.

[23] I. Kamwa, Performance of Three PSS for Interarea Oscillations. [Online]. Available: http://www.mathworks.com/products/simpower/demos.html?file=/products/demos/shipping/powersys/power_PSS.html.

[24] J. F. Hauer, W. A. Mittelstadt, K. E. Martin, J. W. Burns, H. Lee, J. W. Pierre, and D. J. Trudnowski, "Use of the WECC WAMS in wide-area probing tests for validation of system performance and modeling," *IEEE Trans. Power Syst.*, vol. 24, no. 1, pp. 250–257, Feb. 2009.

[25] J. W. Pierre, D. J. Trudnowski, and M. K. Donnelly, "Initial results in electromechanical mode identification from ambient data," *IEEE Trans. Power Syst.*, vol. 12, no. 3, pp. 1245–1251, Aug. 1997.

[26] R. W. Wies, J. W. Pierre, and D. J. Trudnowski, "Use of ARMA block processing for estimating stationary low-frequency electromechanical modes of power systems," *IEEE Trans. Power Syst.*, vol. 18, no. 1, pp. 167–173, Feb. 2003.

[27] N. Zhou, J. W. Pierre, D. J. Trudnowski, and R. T. Guttromson, “Robust RLS methods for online estimation of power system electromechanical modes,” *IEEE Trans. Power Syst.*, vol. 22, no. 3, pp. 1240–1249, Aug. 2007.

[28] N. Zhou, D. J. Trudnowski, J. W. Pierre, and W. A. Mittelstadt, “Electromechanical mode online estimation using regularized robust RLS methods,” *IEEE Trans. Power Syst.*, vol. 23, no. 4, pp. 1670–1680, Nov. 2008.

[29] M. Xiao-ming, Z. Yao, G. Lin, and W. Xiao-chen, “Coordinated control of interarea oscillation in the China Southern power grid,” *IEEE Trans. Power Syst.*, vol. 21, no. 2, pp. 845–852, May 2006.

[30] C. Lu *et al.*, “Wide-area coordinated and adaptive damping control of multiple HVDC links in China Southern Power Grid,” in *Proc. CIGRE 2010 Session*, Paris, France, 2010.

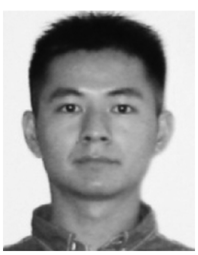

Junbo Zhang (S’10) was born in Guizhou, China, on March 16, 1986. He received the B.Eng. degree (with First Class Honors) from Tsinghua University, Beijing, China, in 2008, where he is currently pursuing the Ph.D. degree.

He studied at The Hong Kong Polytechnic University from 2009 to 2011 under a collaborative program between Tsinghua University and The Hong Kong Polytechnic University. His research areas include wide-area based power system identification and damping control.

C. Y. Chung (M’01–SM’07) received the B.Eng. degree (with First Class Honors) and the Ph.D. degree in electrical engineering from The Hong Kong Polytechnic University, Hong Kong, China, in 1995 and 1999, respectively.

After his Ph.D. graduation, he worked in the Department of Electrical and Computer Engineering at the University of Alberta, Edmonton, AB, Canada, and Powertech Labs, Inc., Surrey, BC, Canada. Currently, he is the Convener of the Power Systems Research Group and an Associate Professor in the Department of Electrical Engineering, The Hong Kong Polytechnic University. His research interests include power system stability/control, planning and operation, computational intelligence applications, and power markets.

Dr. Chung was the Chair of the IEEE Hong Kong Joint Chapter of PES/IAS/PELS/IES in 2007–2009. During his tenure as Chair, the Joint Chapter received the 2008 IEEE PES Outstanding Small Chapter Award and the 2009 IEEE IAS Outstanding Small Joint Chapter Award. He was the Technical Chairman of IET APSCOM2009 International Conference, and Honorary Secretary of IEEE DRPT2004 International Conference and IEEE IAS 2005 Annual Meeting. Currently, he is the Chair of the IEEE Hong Kong Section.

Yingduo Han (SM’95) was born in Shenyang, China, in 1938. He received the B.S. and M.S. degrees from the Electrical Engineering Department, Tsinghua University, Beijing, China, in 1962 and 1965, respectively, and the Ph.D. degree from Erlangen University, Erlangen, Germany.

He is a Professor in the Electrical Engineering Department, Tsinghua University, and was the Vice-Chairman and Chairman of the Electrical Engineering Department from 1986 to 1995. Since 1989, he has been the Head of the Power Electronics Research Center, Tsinghua University. He is a Visiting Professor at the University of Macau, Macau, China. He has published two books and more than 100 papers. He has been engaged for more than 30 years in education and research work on electric power systems and automation. In recent years, he has engaged in FACTS and DFACTS, intelligent control, regional stability control, new dynamic security estimation, and GPS based control systems.

Dr. Han has received four State-level prizes, and six first and second ranked Province-level and Ministry-level prizes. He is a Member of the Chinese Academy of Engineering.